

Identification of Small Molecule Inhibitors that Distinguish between Non-Transferrin Bound Iron Uptake and Transferrin-Mediated Iron Transport

Jing Xu Brown, Peter D. Buckett,
and Marianne Wessling-Resnick*
Harvard School of Public Health
Department of Genetics and Complex Diseases
665 Huntington Avenue
Boston, Massachusetts 02115

Summary

Chemical genetics is an emerging field that takes advantage of combinatorial chemical and small molecule libraries to dissect complex biological processes. Here we establish a fluorescence-based assay to screen for inhibitors of iron uptake by mammalian cells. Using this approach, we screened the National Cancer Institute's Diversity Set library for inhibitors of non-transferrin bound iron uptake. This screen identified 10 novel small molecule inhibitors of iron transport with IC_{50} values that ranged from 5 to 30 μ M. Of these ten compounds, only two blocked uptake of iron mediated by transferrin. Thus, this study characterizes the first small molecule inhibitors that distinguish between different pathways of iron transport.

Introduction

Classical genetics is based on determining phenotypic changes that result from mutation of genes and ordering those identified genes into functional pathways. By analogy, the emerging field of chemical genetics takes advantage of small molecule libraries to dissect complex biological processes [1–3]. Past use of small molecule antagonists typically entailed “reverse genetics” to conditionally eliminate protein function and on that basis to subsequently identify the target for inhibition. Studies of carrier-mediated transport to learn how nutrients, ions, and other factors enter or exit cells have often relied on such small molecule inhibitors: the cardiac glycoside ouabain (an inhibitor of the Na-K ATPase), the antibiotic cytochalasin B (an inhibitor of glucose transport), and the diuretic amiloride (an inhibitor of epithelial Na channels) are just a few well-established examples. These natural products were either fortuitously discovered [4, 5] or actively sought as pharmacological antagonists of transporter function [6] and were instrumental in the analysis of transport mechanisms [4, 7, 8], the identification of the molecules involved [9–13], and in some instances, the elucidation of functionally important domains [14–16]. There is a need, however, to develop “forward chemical genetics” to discover new small molecules that interact with key elements in a pathway of interest. Thus, the basis for forward chemical genetics is a phenotypic screen of small molecule libraries such that one can identify inhibitory (or stimulatory) effects by observing a change in cellular properties.

One very important area of nutrient transport lacking pharmacological reagents for advanced study concerns the uptake of iron. A commonly recognized pathway for iron uptake by mammalian cells is through receptor-mediated endocytosis of transferrin (Tf). Once internalized with its receptor, diferric Tf is delivered to endosomes wherein iron is released due to the low pH of this compartment [17]. Mechanistically, transport of iron released from Tf across endosomal membranes is thought to involve the reduction of Fe(III) to Fe(II) [18–20], but the actual iron-translocating machinery has yet to be rigorously defined. A strong candidate membrane carrier has emerged called DMT1 [21]. Divalent Metal Transporter 1 (DMT1, also known as DCT1 and Nramp2) is known to be involved in iron assimilation, since defects in its gene promote microcytic anemia in the *mk* mouse, a genetic model with defective dietary iron absorption [22]. The functional activity of DMT1 has been characterized using exogenous expression in *Xenopus* oocytes [23]. In addition to its function in Fe(II) uptake, a role for DMT1 in assimilation of iron from Tf was elucidated by the discovery that its gene is also mutated in the Belgrade rat [21]. Defects in Tf-mediated iron uptake are well characterized for this animal model [24–26]. Tf is internalized by Belgrade rat reticulocytes, but its cargo iron fails to be captured because of a loss of transmembrane transport activity in the endosome [27, 28]. The observation that the pH-dependent DMT1 transporter localizes to acidic endosomal compartments further supports its role in this process [29, 30]. However, direct functional evidence to fully support this model is lacking, and how ferric iron is reduced after its release from Tf to make substrate available for DMT1 transport is still unknown. Furthermore, although Tf-mediated iron uptake is a more widely recognized process, most cells also import nontransferrin bound iron (NTBI) presented as Fe(III) chelates [31–37]. The latter pathway plays a key role in the pathology of hemochromatosis since NTBI is found in serum from patients with this and other iron-overload disorders [38]. NTBI uptake does not involve endocytic membrane traffic [32], and apparent K_m values for transport have been reported between 0.5 and 20 μ M, falling in the range of serum NTBI concentrations in patients with iron overload [38, 39]. Characterization of this process indicates that it also most likely involves ferrirreduction of Fe(III) to Fe(II), but the mechanistic details of NTBI uptake are rather obscure [31]. It is possible that DMT1 functions in the import of NTBI from plasma, but this possibility has not been directly tested.

As a first step to determine mechanistic elements that may be unique to each of these iron transport pathways, we sought to identify small molecule inhibitors that selectively inhibit NTBI uptake. To initiate the discovery process, we have established a fluorescence-based assay useful for medium throughput screening of iron transport inhibitors. Here we demonstrate the utility of this chemical genetics approach by identifying ten novel iron uptake inhibitors determined to block NTBI uptake.

*Correspondence: wessling@hsph.harvard.edu

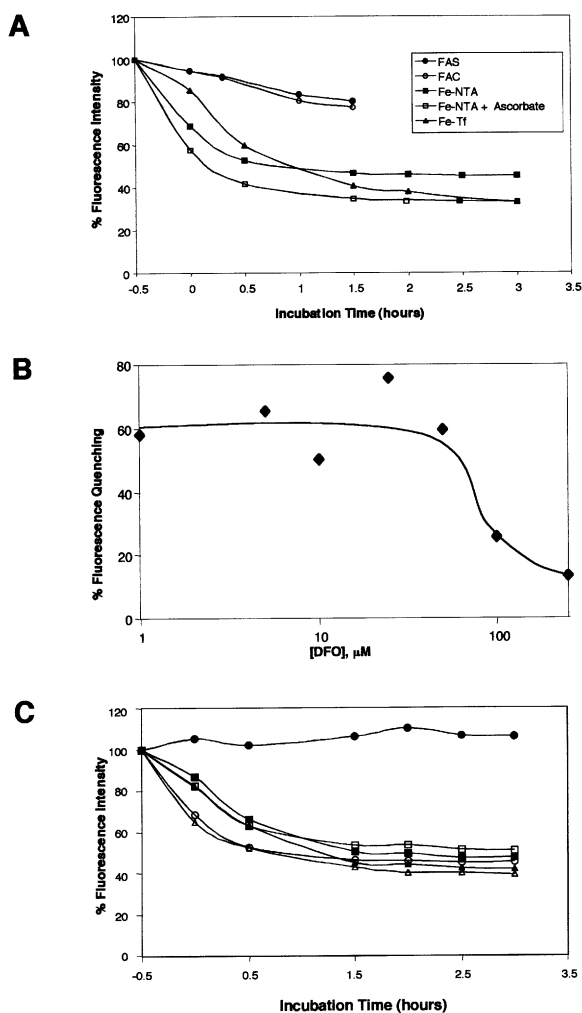


Figure 1. Development of a Cell-Based Fluorescence Assay for Iron Uptake

(A) Comparison of the ability of different iron sources to induce changes in the intracellular labile iron pool as assayed by calcein fluorescence quenching. HeLa cells (1500) were seeded into each well of a 384-well plate, grown overnight, then washed 5 times with serum-free and phenol red-free DMEM and incubated with 0.25 μM calcein AM for 1 hr. After loading with the fluorophore, cells were washed 10 times with HBSS and were subsequently incubated with 150 μM FAS (filled circles) or FAC (open circles), or 100 μM Fe-NTA (filled squares), 100 μM Fe-NTA + Ascorbate (open squares), or 100 μM Fe-Tf (triangles) in 50 μl HBSS for times indicated. The fluorescence intensity (excitation 485 nm; emission 535 nm) of each well was measured before and after incubation with different iron sources to calculate the % change in fluorescence intensity as a function of time.

(B) Iron chelation by DFO blocks calcein fluorescence quenching by Fe-NTA. HeLa cells were cultured and loaded with calcein as described for (A) except that prior to addition of 100 μM Fe-NTA, cells were pretreated with 0–500 μM DFO in HBSS for 1 hr. The fluorescence intensity was then measured before and after incubation with 100 μM Fe(NTA)₃ for 3 hr. The difference in fluorescence intensity due to quenching was normalized to control (no treatment) and is plotted as a function of inhibition by [DFO]. Shown are mean values determined for triplicate samples.

(C) Time course of calcein fluorescence quenching. HeLa cells were plated onto 384-well plates to determine the time course of fluorescence quenching exactly as described above except that incubations were carried out in the absence (filled circles) or presence of

Of these ten compounds, only two perturb Tf-mediated iron assimilation, supporting the selectivity of the other eight in blocking NTBI uptake. These reagents therefore provide new chemical tools to help distinguish between NTBI uptake and Tf-mediated iron transport and to enable further characterization of the determinants unique to both processes at the molecular level.

Results

A Fluorescent Cell-Based Assay to Screen for Small Molecule Inhibitors of Transport

To advance the study of iron transport through chemical genetics, we established a fluorescence-based uptake assay utilizing a 384-well format for medium-throughput screening. Conceptually based on work by Cabantchik and colleagues [40], the assay employs the metal-sensitive fluorophore calcein to measure intracellular “labile” or free iron. Iron taken up by cells transits the so-called labile iron pool before deposition in ferritin (for storage) or uptake by mitochondria (for metabolism). Calcein has been used by several different groups to determine the size of the labile iron pool under various conditions [41–45]. Calcein fluorescence is quenched when iron or other metals are bound [40]. Because calcein fails to bind calcium or magnesium ions at physiological pH and the intracellular concentration of other metals is relatively low, a decrease in cell-associated calcein fluorescence in the presence of an extracellular source of iron provides a relative measure of increased free intracellular iron content due to iron uptake [40, 41]. For our studies, we employed an acetomethyl ester of calcein (calcein-AM). Upon entering cells, cellular esterases cleave this compound, leaving the membrane impermeant fluorophore resident inside cells with very little leakage as long as cellular integrity is maintained. The loss of fluorescence signal when iron is transported into cells reports an increase in the cellular free iron pool, as assessed by the extent of fluorescence quenching. A key advantage of this approach is that calcein fluorescence also provides an indicator of cell viability such that the loss of fluorescent signal in the presence of a drug but in the absence of iron reports the toxicity and/or fluorescence properties of that compound (see below).

Preliminary analysis examining calcein quenching in HeLa cells in response to iron uptake indicated that an appropriate determination could be made using 0.25 μM calcein to load these cells (signal \sim 8-fold higher than background). There was no substantial interference from calcein-loading into nonviable cells (data not shown). Similarly, buffering, washing, and iron-loading conditions were each carefully examined. Studies using HBSS yielded optimal signal-to-noise ratios, and a minimum of 8 separate wash steps were required to eliminate extracellular fluorophore (detected by quenching of extracellular calcein using Trypan blue). Figure 1A demonstrates that under these carefully optimized con-

different concentrations of Fe-NTA: 10 μM (filled squares); 25 μM (filled triangles); 50 μM (open squares); 75 μM (open triangles); and 100 μM (open circles).

ditions, calcein-loaded HeLa cells display a time-dependent fluorescent quenching in the presence of various substrates for iron transport. Using this assay, uptake of iron from Tf, transport of NTBI (provided to cells as Fe-NTA), and uptake ferrous iron (reduced in the presence of ascorbate) were measured. Maximal quenching was observed by 2 hr for each of these transport substrates. Ferric ammonium sulfate (FAS) and ferric ammonium citrate (FAC), which are less bioavailable forms of iron, did not quench the calcein signal as strongly.

To confirm that calcein fluorescence quenching was due to iron uptake, the iron-specific chelator desferrioxamine (DFO) was introduced during transport incubations along with Fe-NTA. As shown in Figure 1B, DFO blocked the quenching effect observed in the presence of 100 μM Fe-NTA, providing a “positive” control to screen for inhibitors of iron uptake since inhibition by 100 μM DFO was essentially complete. Finally, to confirm that the change in fluorescence signal was dose responsive to extracellular iron concentration, a series of experiments that measured the time course of uptake was performed using 10 to 100 μM Fe-NTA (Figure 1C). Based on the results summarized in Figure 1, parameters for uptake studies were optimized to screen for inhibition of iron uptake using Fe-NTA at 100 μM with a 2 hr incubation at 37°C to achieve maximal uptake and calcein fluorescence quenching.

Screen of the NCI Diversity Set Library Identifies Potent Inhibitors of NTBI Uptake

Using the fluorescent cell-based iron uptake assay, we surveyed the NCI Diversity Set library for inhibitors of iron uptake because of its relatively small size (~ 2000 compounds) and molecular attributes (i.e., structurally represents a finite set of pharmacophores). Further information about the NCI Diversity Set is available at http://dtp.nci.nih.gov/branches/dscb/diversity_explanation.html. A pin-transfer robotic system was used to administer the compounds, permitting the transfer of fixed 10 nl aliquots from the small molecule library stocked at 10 mM compound in DMSO and provided by Harvard Medical School Institute of Chemistry and Cell Biology (ICCB). Two independent pin-transfers were used for screening at a final nominal concentration of 40 μM . The rationale for this concentration of drug was that effective delivery of some compound could be assured (2 rounds of transfer) while strong iron chelators might be avoided in the selection process: e.g., 100 μM Fe-NTA is effectively blocked by 100 μM DFO but not 40 μM DFO (Figure 1B). We reasoned that similar iron chelators present in the library would be substoichiometric and score only as “weak” inhibitors. Based on the transport assay conditions established above, the screening protocol was adopted as follows: step 1, plate 1500 HeLa cells/well on 384-well clear-bottom plates and allow cells to attach overnight; step 2, wash cells twice, add 0.25 μM calcein-AM, briefly centrifuge plates, and incubate for 1 hr at 37°C; step 3, wash cells 8 times (twice in succession) with HBSS; step 4, measure initial fluorescence (F_0); step 5, robotically pin-transfer test compounds or DFO controls, briefly centrifuge plates, and incubate for 30 min at 37°C; step 6, measure fluores-

cence once again (F_d), add Fe-NTA (100 μM final concentration), and incubate 2 hr at 37°C; and step 7, measure fluorescence for a final reading (F_f).

During the screen, fluorescence measurements were compiled to calculate a viability and drug fluorescence index or $(F_d - F_0)/F_0$; this ratio for control cells (incubated in the absence of any addition except vehicle DMSO) routinely fell within $\pm 5\%$ – 10% . Values for wells treated with drug that were less than -10% (loss of signal or apparent “quench”) indicated that the compound was toxic such that cell viability was compromised or that the drug itself quenched calcein fluorescence. Values greater than $+10\%$ indicated that the drug was fluorescent when excited at 485 nm. Thus, use of the viability and drug fluorescence index eliminated potential artifacts in the screening process. The viability and drug fluorescence values were compared against inhibition/activation values or $(F_d - F_f)/F_d$ to eliminate these “false positives.” The $(F_d - F_f)/F_d$ ratio of negative control cells (incubated with Fe-NTA but no DFO in the absence of any compound) was $\sim -60\%$ under our optimized assay conditions. The values for positive control cells (incubated with Fe-NTA in the presence of DFO) was $\sim 0\%$. Thus, any change between 0% and 60% indicated that a compound inhibited uptake of Fe-NTA by HeLa cells. In implementing this screening protocol, well-to-well and plate-to-plate variations were recognized that made it difficult to compare these calculated values across the entire NCI Diversity Set (contained in seven 384-well plates). It was necessary to develop a mechanism to normalize across the library to directly compare potencies. For final analysis, the inhibition/activation ratio was normalized by setting the average $(F_d - F_f)/F_d$ ratio of 15 independent wells for negative control cells (calcein alone) to “0” as F_{min} , and the average $(F_d - F_f)/F_d$ ratio of 15 independent wells for positive control cells (calcein with Fe-NTA) to “1” as F_{max} for each individual plate. The adjusted inhibition/activation values were then calculated as $(F_f - F_{\text{min}})/(F_{\text{max}} - F_{\text{min}})$.

To validate candidates, the entire NCI Diversity Set library was screened twice under identical conditions. Pooled data were carefully examined to eliminate non-specific effects (i.e., intrinsic fluorescence, cell toxicity) and to ensure reproducibility of strong inhibitory effects. Ten compounds met these criteria with the structures shown in Table 1. These compiled data represent a “hit rate” of $\sim 0.5\%$, supporting the selectivity of the assay for specific inhibitors. Samples of each of these compounds were subsequently obtained from Dr. Robert J. Schultz, Drug & Chemistry Synthesis Branch at NCI; drug reference numbers from the NCI Diversity Set are given in Table 1. Each inhibitor was rescreened for the ability to inhibit Fe-NTA uptake using the calcein method, and dose response curves were constructed (Figure 2; derived IC_{50} values are shown in the table). IC_{50} values ranged from 5 to 30 μM , but several compounds were found to be cytotoxic as indicated by the reversal of quenching and/or enhanced fluorescence (loss of cell viability) at higher concentrations (see atypical “J” curves for 56M19, 56N16, 57H10, 56N08). While this observation does not necessarily exclude the future utility of these inhibitors, it does caution about the nature of these particular small molecules.

Table 1. Inhibitors of NTBI Transport

Plate ID	NCI #	IC ₅₀	Structure	Comments
57N19	11079	5 μm		Inhibits both NTBI and Tf-mediated iron uptake
54C20	34908	20 μm		Structurally related to antifertility and anoxia agents
54N20	75600	20 μm		GABA receptor ligand analog
56N08	48874	>10 μm		Toxic >20 μm; ACS Registry # 6640-40-0
56N16	48010	12 μm		Toxic >20 μm
55L06	306711	5 μm		Inhibits both NTBI and Tf-mediated iron uptake
55B05	331973	10 μm		Toxic? >30 μm
56I18	27236	25 μm		Benzoic acid; chemical etching agent; derivatives have fungal and antibacteriocidal activity; metal binding?
57H10	124808	30 μm		Toxic >50 μm; commercially available from Ambinter; metal ligand binding?; antipsychotic hypnotic activities in structurally related compounds
56M19	13831	>15 μm		Toxic >40 μm

Database searches of the CAS (Chemical Abstract Services) Registry, MEDLINE searches of the National Library of Medicine, and searches of the American Chemical Society (ACS) Registry of Compounds were

conducted for information on the same or structurally related compounds using the SciFinder Scholar search engine. Several compounds (54C20, 54N20, 56I18, 57H10) have been previously studied with comments

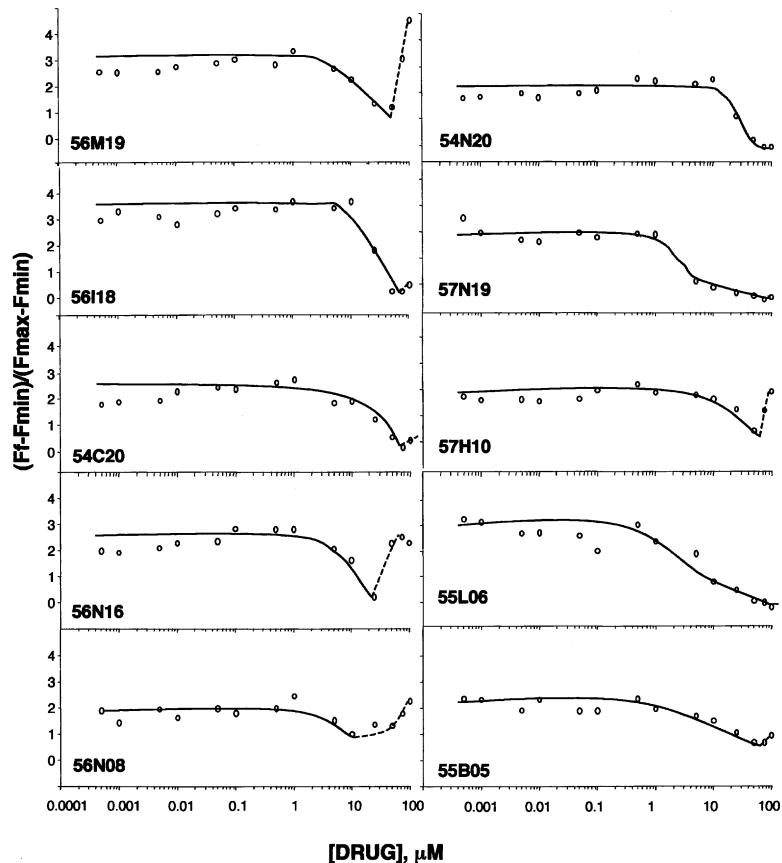


Figure 2. Dose-Response Studies of Potent NTBI Inhibitors

Inhibitory compounds listed in Table 1 were obtained from Dr. Robert J. Schultz, Drug & Chemistry Synthesis Branch at NCI and retested for the ability to block uptake of iron using the 384-well assay described in the text with final concentrations between 0.5 nM and 100 μ M. Average fluorescence values of triplicate samples were used to determine $(F_f - F_{min})/(F_{max} - F_{min})$ and plotted against inhibitor concentration.

listed in Table 1. Others (56N08) were found in the ACS Registry but with no further details, and for the rest we were unable to find any information. None of the compounds have been previously associated with cellular iron transport.

Characterization of Transport Inhibitors Distinguishes Mechanistic Differences between NTBI Uptake and Tf-Mediated Iron Assimilation

One of the immediate questions we addressed using this set of inhibitors was whether they perturbed uptake of iron from Tf. Although some of the properties of NTBI uptake and Tf-mediated iron assimilation appear similar (e.g. ferrireduction followed by membrane translocation), reaction conditions are quite different (e.g., uptake across endosomal membrane at acidic pH versus transport at the cell surface at neutral pH). Initially, the ten inhibitors were screened at 50 μ M for effects on Tf bound iron (Tf-Fe) uptake (Figure 3). Briefly, HeLa cells were incubated with the small molecules for 4 hr at 37°C (filled bars) or 4°C (open bars) in the presence of 13 nM ^{55}Fe -Tf. ^{55}Fe uptake was quenched by chilling the cells on ice and incubating with 40 μ M unlabeled Fe-Tf for 1 hr to any displace surface bound radiolabel [46, 47]. Cell lysates were collected to measure cell-associated radioactivity and protein content to calculate pmol Fe/mg protein as shown. Significant differences ($p < 0.05$) are indicated by an asterisk. Of the ten compounds

tested, only two (57N19 and 55L06) had significant effects on TBI.

Characterization of 57N19 and 55L06 Inhibition of Tf-Mediated Iron Uptake

The dose response for inhibition of Tf-mediated iron uptake was examined for the two compounds that had significant inhibitory effects, 57N19 and 55L06 (Figure 4). IC_{50} values of ~ 63 and 20 μ M, respectively, were determined from this analysis. To test the reversibility of inhibition, cells were first treated either with 55L06 or 57N19 for 2 hr or with both compounds for 1 hr, followed by a 2 hr recovery period with vehicle (DMSO) added. Inhibition of Tf-mediated iron uptake and NTBI transport were both reversed under the latter conditions (Figure 5). These results confirmed that neither compound is toxic to cells.

Discussion

This report establishes a cell-based screening method that enables rapid identification of transport inhibitors with concurrent detection of cytotoxicity. Using calcein fluorescence quenching as a measure of iron uptake [40], we exploited use of this reagent as a vital stain for cell viability [48, 49]. By establishing initial measurements for the viability and drug fluorescence index $[(F_d - F_o)/F_o]$, we were able to immediately identify those compounds exerting toxic effects, as well as those

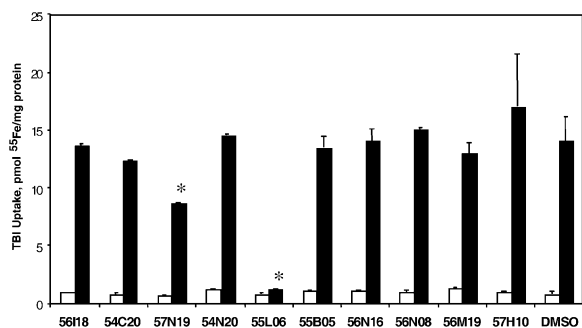


Figure 3. Effect of Inhibitors on Transferrin Bound Iron Uptake
HeLa cells were incubated with 50 μM of the indicated compounds for 4 hr at 37°C (filled bars) or 4°C (open bars) in the presence of 13 nM ^{55}Fe -Tf. ^{55}Fe uptake was quenched by chilling the cells on ice and incubating with 40 μM unlabeled Fe-Tf for 1 hr to displace surface bound ^{55}Fe -Tf; lysates were collected to measure cell-associated radioactivity and protein content to calculate pmol Fe/mg protein. Shown are the means \pm SD with significant differences ($p < 0.05$) indicated by an asterisk. Data were analyzed using ANOVA and Fisher's post hoc test.

with interfering intrinsic fluorescence or quenching properties. This approach streamlined our survey of normalized inhibition/activation values $[(F_f - F_{\text{min}})/(F_{\text{max}} - F_{\text{min}})]$ by eliminating potential small molecule inhibitors with these nonspecific effects, ensured the reproducibility of results, and led to immediate confirmation of the most potent effectors. From our screen of the NCI Diversity Set library, 10 small molecule inhibitors that blocked iron-induced calcein fluorescence quenching were selected for further study based on these stringent criteria. It should be noted that in our screen of this library many “activators” of iron uptake were also concurrently identified. These compounds could promote iron absorption through a variety of different effects; for example, by altering cell permeability to enhance iron uptake or by reducing iron to render it more bioavailable for transport. Since iron-deficiency anemia is an important problem worldwide [31], the discovery of activators of iron transport is certainly not without merit and warrants future consideration. However, our primary intent in this investigation was to discover inhibitors of NTBI uptake in order to establish pharmacological reagents to aid in molecular analysis of the mechanistic elements involved in iron transport.

Ten small molecule inhibitors of NTBI uptake were discovered in this screen with diverse structural features (Table 1). We can not find any reports exploring their possible influences on these chemicals on iron transport, and only two of the ten inhibited Tf-mediated uptake. Five (56N08, 56N16, 55B05, 57H10, and 56M19) were cytotoxic at higher concentrations, suggesting that the usefulness of these compounds and derivatives for cell-based studies may be limited. It is unlikely that their cytotoxicity is related to interference of iron uptake over the time frame of our experiments since cellular iron depletion by strong chelators like DFO requires many hours, if not days, to promote cell death. Three compounds (54C20, 54N20, and 56118) are more attractive candidates for future follow-up studies. Although 56118 (benzoic acid) has metal binding properties, its IC_{50} for

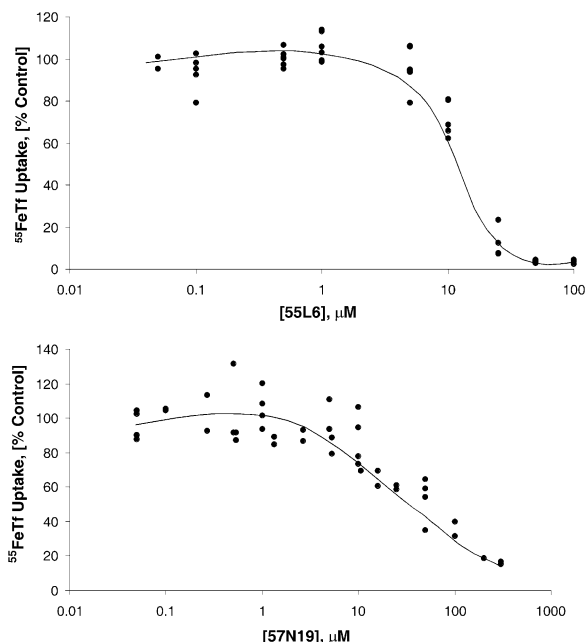


Figure 4. 55L06 and 57N19 Inhibit Tf-Mediated Iron Uptake in a Dose-Dependent Manner

HeLa cells were incubated with 0.05–300 μM 55L06 (top) and 57N19 (bottom) in the presence of 13 nM unlabeled ^{55}Fe -Tf for 4 hr at 37°C. Cells were chilled on ice, incubated with 40 mM unlabeled Tf to displace any ligand bound iron associated with the cell surface, and then washed. Iron uptake was determined as described for Figure 3 and normalized to control (vehicle alone). Data shown are pooled from three independent experiments measuring % inhibition for each compound.

transport inhibition (25 μM) is much lower than the concentration of Fe-NTA used in our study (100 μM), and it is therefore unlikely that this compound acts to block uptake via iron chelation. Benzoic acid derivatives have, however, been used extensively as chloride channel blockers [50]. In this regard, it is of particular interest that 54C20 (5-phenyl-2-pyrrole propionic acid or PPP) is a γ -aminobutyric acid (GABA) analog since stimulation of GABA receptors results in increased chloride conductance [50–52]. A role for chloride channels in yeast iron transport and metabolism has been identified [53], and our observations therefore prompt the idea that mammalian iron transport may also be coupled to this function. Experiments are underway to test this possibility and to further explore the mechanism of action for the other more potent inhibitor of NTBI uptake, 54N20.

The idea that common mechanistic elements may exist between NTBI and Tf-mediated iron uptake is supported by the discovery of 57N19 and 55L06. Both inhibitors act in a dose-dependent manner to block NTBI and Tf-mediated iron uptake. However, the IC_{50} values for inhibition of the latter process are about an order of magnitude greater (63 and 20 μM , respectively) than their IC_{50} for inhibition of NTBI uptake (~ 5 μM for each compound). This difference could be a consequence of low cellular permeability since they would both presumably need to access intracellular endosomal compartments to exert direct functional effects on the transport

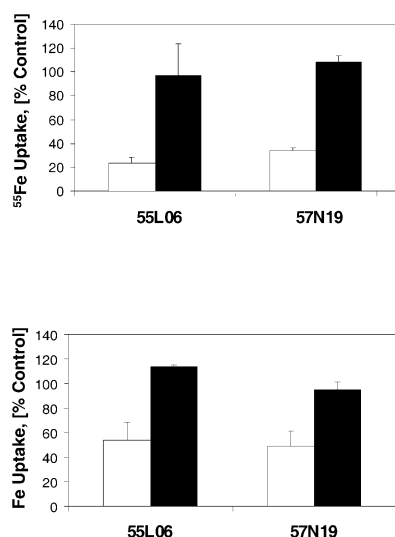


Figure 5. 55L06 and 57N19 Inhibit Iron Uptake in a Reversible Manner

To determine the reversibility of inhibition of Tf-mediated iron uptake (top), HeLa cells were incubated at 37°C with 20 μ M 55L06 or 100 μ M 57N19 for 1 hr, followed either by a 2 hr recovery period (filled bars) or by continued 1 hr incubation in the presence of the drug (open bars). ⁵⁶Fe-Tf (13 nM) was then added for a further 2 hr incubation to determine iron uptake. Uptake was quenched by chilling the cells on ice and incubating with 40 μ M unlabeled Fe-Tf for 1 hr to displace surface bound ⁵⁶Fe-Tf; lysates were collected to measure cell-associated radioactivity and protein content. ⁵⁶Fe uptake was normalized to protein content and expressed as % of control (DMSO alone). To test the reversibility of NTBI uptake inhibition (bottom), HeLa cells were incubated at 37°C with 0.25 μ M calcein for 1 hr. After extensive washing, cells were incubated with 5 μ M 55L06 or 57N19 with and without a recovery period as described above. Reversibility of fluorescence quenching was determined as % control (DMSO alone).

of iron released from internalized Tf. Alternatively, these compounds may be catabolized such that their efficacy is lost once they penetrate cells. The process of Tf-mediated iron uptake also involves additional steps that are unique from NTBI transport. For example, 57N19 or 55L06 could block endocytosis, the release of iron from Tf, or recycling of Tf receptors to the cell surface. Therefore, it is possible that differences in the IC₅₀ values reflect differences in the mechanism of action of the compounds on Tf-mediated uptake. While further studies are clearly necessary to determine what specific effects 57N19 and 55L06 have on the Tf receptor pathway, the fact that certain features of NTBI and Tf-mediated iron uptake are similar (e.g., requirement for ferrireduction) supports the simpler model that these small molecule inhibitors may act on mechanistic elements that are common to both pathways.

Our identification of this set of small molecule inhibitors greatly expands the repertoire of pharmacological reagents to study iron transport. To date, molecules that have been characterized to inhibit uptake function as iron chelators, like DFO. DFO chelates NTBI in a 1:1 complex to block uptake, but does not release iron from Tf and therefore does not directly interfere with Tf-mediated transport. To the contrary, cells depleted of iron by DFO upregulate the number of Tf receptors in re-

sponse to their iron deficiency. Other chelators, like diethylenetriaminepentaacetic acid (DTPA), do not have the same metal selectivity as DFO for iron and therefore can exert pleiotropic effects. A class of compounds that has proven useful in studies of cellular iron metabolism are pyridoxal isonicotinoyl hydrazone (PIH) and its analogs [54, 55]. These compounds bind iron in a 2:1 complex and can actually deliver the metal to cells such that proliferation is supported. These chelators also do not remove iron from Tf but have been shown to mobilize iron from cells after uptake by the Tf-mediated pathway, serving as a shuttle to move the metal out of cells. Thus, although they complex iron, the metal is still available for cellular metabolism. A relatively new chelator, ICL670A, which also binds iron in a 2:1 complex, is currently in clinical trials for therapeutic use in iron chelation, but little is known yet about its effects at the cellular level [56]. In contrast to these chelating reagents, the ten inhibitors identified in the NCI diversity set screen are unlikely to block uptake by complexing iron. Some may possibly exert indirect effects, as we speculate 54C20 and 56I18 might act on counter-ion flux to disrupt iron uptake. Others (e.g., 54N20) may selectively interact with molecules involved in membrane translocation of NTBI. Finally, 57N19 and 55L06 might interfere with elements common between NTBI and Tf-mediated iron uptake pathways.

We hope that future use of these chemical tools will yield important insights into characteristics of NTBI and/or Tf-mediated iron uptake that will ultimately lead to target identification. The development of the calcein fluorescence quenching method to screen for inhibitors of these pathways establishes the necessary basis for further discovery of additional small molecule inhibitors of iron transport. Our future efforts in chemical genetics will not only focus on the mechanistic characterization of the inhibitors identified in this screen, but will also center on additional screening of different chemical libraries for inhibitors of both NTBI and Tf-mediated iron uptake.

Significance

Chemical genetics is an emerging field that takes advantage of small molecule libraries to dissect complex biological processes. Past use of small molecule antagonists typically entailed “reverse” chemical genetics to conditionally eliminate protein function, and on that basis to identify the target of inhibition. Studies of carrier-mediated transport to learn how nutrients, iron, and other factors enter or exit cells have relied heavily on the use of such pharmacological reagents, and among many well-established examples are the use of ouabain to study the Na-K ATPase, of cytochalasin B to inhibit glucose transport, and of derivatives of the diuretic amiloride to identify and purify Na channels. There is a need, however, to develop “forward” chemical genetics approaches to discover small molecules that interact with key elements in a pathway of interest. Forward chemical genetics must be based on a phenotypic screen of small molecule libraries such that one can identify effectors by observing a

change in cellular properties. One important area of nutrient transport studies lacking pharmacological reagents for advanced study concerns iron uptake. In this report, we establish the basis for a cell-based forward chemical genetics screen. Our approach is unique in that it enables rapid identification of transport inhibitors with the concurrent detection of cytotoxicity of the compounds screened. Using this fluorescence-based method, we have screened the National Cancer Institute Diversity Set library to discover ten novel small molecule inhibitors of non-transferrin bound iron uptake. Only two of these compounds blocked iron uptake via transferrin-mediated transport, thus establishing the first pharmacological tools that distinguish different pathways of cellular iron absorption.

Experimental Procedures

Fluorescence-Based Assay for the Uptake of Iron by HeLa Cells as Detected by Changes in the Labile Iron Pool

Details of the development of this screening assay are described more fully in the text. For screening purposes, 1500 HeLa cells were seeded into each well of seven 384-well plates (except wells of column 24) and cultured overnight in Dulbecco's minimal essential medium (DMEM) containing 10% fetal bovine serum. Unless otherwise indicated, cells were incubated at all times in a humidified environment with 5% CO₂ at 37°C. A 384-well plate has 24 columns and 16 rows labeled 1–24 and A–P, respectively. On the second day, cells were washed twice with DMEM, and calcein AM was added to each well with a final concentration of 0.25 μM calcein-AM. After a 1 hr incubation, cells were washed 16 times with Hank's buffered saline solution (HBSS). Subsequently, compounds from National Cancer Institute (NCI) Diversity Set arrayed in 384-well plates were transferred to the corresponding wells containing HeLa cells in 40 μl HBSS using a pin-transfer robotic system. This small molecule library was provided by Harvard Medical School's Institute for Chemistry and Cell Biology (ICCB) with 10 mM stocks for each compound contained in 384-well plates (ICCB numbering plates 53–59). After delivery, the nominal final concentration in each well was estimated to be 40 μM. At this time of addition, the iron chelator desferrioxamine (DFO) was also added to wells in columns 23 and 24 to achieve a final concentration of 100 μM. Cells were incubated with compounds and/or DFO for 30 min, then 100 μM Fe-NTA (1:4 chelate ratio) was added to wells in columns 2–24 and incubation was continued for 2 hr. The fluorescence intensity excitation 485 nm; emission 535 nm) of each well was measured before (Fo) and after (Fd) incubation with compounds or DFO and was also measured after incubation with 100 μM Fe-NTA (Ff). All of the wells in column 1, which only contain HeLa cells incubated with calcein AM but not DFO nor Fe-NTA, were included as negative controls, since intrinsic fluorescence should not be quenched by the uptake of iron in absence of the fluorophore. All the wells in column 2, which contain HeLa cells incubated with Fe-NTA but not DFO, were used as positive controls for calcein fluorescence that was quenched by uptake of iron. All of the wells in column 23, which contain HeLa cells incubated with calcein AM, DFO, and Fe-NTA, were used as positive controls for inhibition of iron uptake and calcein fluorescence quenching. All of the wells in column 24, which contain calcein AM, DFO, and Fe-NTA, but no cells, were used as blanks.

The (Fd – Fo)/Fo ratios of control cells with no DFO nor Fe-NTA (column 1) fell within ±10%. Therefore, fluorescence quenching greater than 10% indicated that a drug might bind iron or that it might be fluorescent itself. Less than –10% indicated that a drug was toxic such that cell viability was compromised. The (Fd – Ff)/Fd ratio of negative control cells (column 2 incubated with Fe-NTA but not DFO) was ~40%. The (Fd – Ff)/Fd ratio of positive control cells (column 23 incubated with Fe-NTA and DFO) was ~0%. Any change between 0% and 40%, therefore, indicated that a drug inhibited the uptake of iron by HeLa cells. Because of well-to-well and plate-to-plate variations, to compare the values across the library,

(Fd – Ff)/Fd ratios were normalized by setting the average (Fd – Ff)/Fd ratio (Fmin) of negative control cells with no DFO nor Fe-NTA (column 1) as 0, and the average (Fd – Ff)/Fd ratio (Fmax) of positive control cells with DFO and Fe-NTA (column 2) as 1. The normalized ratio for each well was then calculated as: (Ff – Fmin)/(Fmax – Fmin). All equipment and robotic instrumentation used for screening was provided by facilities at ICCB and is described at <http://iccb.med.harvard.edu>.

Tf-Mediated Iron Transport Assays

HeLa cells were washed with serum-free media and incubated with 13 nM ⁵⁵Fe-Tf at 37°C with or without inhibitors at the concentrations shown in Figure legends. As a control, cells were incubated with vehicle alone (0.5% DMSO). At the end of the uptake period, cells were rapidly chilled on ice, washed twice with ice-cold phosphate-buffered saline containing 1 mM MgCl₂ and 0.1 mM CaCl₂ (PBS⁺⁺), then incubated with 40 μM unlabeled Tf for 1 hr to displace surface bound ⁵⁵Fe-Tf. Cells were washed twice with PBS⁺⁺ and lysed with 600 μl solubilization buffer (0.1% Triton X-100, 0.1% NaOH). Cell-associated radioactivity was determined by liquid scintillation counting and cell protein was measured using the Bradford assay to calculate pmol ⁵⁵Fe/mg cell protein.

Acknowledgments

We thank Jim Follen, Caroline Shamu, Rebecca Ward, and Tim Mitchison at the Harvard Institute for Chemical and Cell Biology for the help and guidance with this project. We are grateful for the use of the ICCB instruments and facilities. We are also indebted to Robert Schultz at the Drug Synthesis & Chemistry Branch, Developmental Therapeutics Program, Division of Cancer Treatment and Diagnosis, National Cancer Institute for his help in procuring test compounds used in this study. This work was supported by National Institutes of Health grants DK56160 and DK55495.

Received: November 5, 2003

Revised: December 23, 2003

Accepted: January 5, 2004

Published: March 19, 2004

References

1. Specht, K.M., and Shokat, K.M. (2002). The emerging power of chemical genetics. *Curr. Opin. Cell Biol.* 14, 155–159.
2. Stockwell, B.R. (2000). Frontiers in chemical genetics. *Trends Biotechnol.* 18, 449–455.
3. Stockwell, B.R. (2000). Chemical genetics: ligand-based discovery of gene function. *Nat. Rev. Genet.* 1, 116–125.
4. Lingrel, J.B., and Kuntzweiler, T. (1994). Na⁺K⁺-ATPase. *J. Biol. Chem.* 269, 19659–19662.
5. Carter, S.B. (1967). Effects of cytochalasins on mammalian cells. *Nature* 213, 261–264.
6. Benos, D.J. (1982). Amiloride: a molecular probe of sodium transport in tissues and cells. *Am. J. Physiol.* 242, C131–C145.
7. Schwartz, A., Grupp, G., Wallick, E., Grupp, I.L., and Ball, W.J., Jr. (1988). Role of the Na⁺K⁺-ATPase in the cardiotoxic action of cardiac glycosides. *Prog. Clin. Biol. Res.* 268B, 321–338.
8. Wardzala, L.J., Cushman, S.W., and Salans, L.B. (1978). Mechanism of insulin action on glucose transport in the isolated rat adipose cell. Enhancement of the number of functional transport systems. *J. Biol. Chem.* 253, 8002–8005.
9. Czech, M.P. (1976). Characterization of (3H)cytochalasin B binding to the fat cell plasma membrane. *J. Biol. Chem.* 251, 2905–2910.
10. Carter-Su, C., Pessin, J.E., Mora, R., Gitomer, W., and Czech, M.P. (1982). Photoaffinity labeling of the human erythrocyte D-glucose transporter. *J. Biol. Chem.* 257, 5419–5425.
11. Sariban-Sohrab, S., and Benos, D.J. (1986). Detergent solubilization, functional reconstitution, and partial purification of epithelial amiloride-binding protein. *Biochemistry* 25, 4639–4646.
12. Kleyman, T.R., Yulo, T., Ashbaugh, C., Landry, D., Cragoe, E., Jr., Karlin, A., and Al-Awqati, Q. (1986). Photoaffinity labeling of the epithelial sodium channel. *J. Biol. Chem.* 261, 2839–2843.

13. Barbry, P., Chassande, O., Vigne, P., Frelin, C., Ellory, C., Cragoe, E.J., Jr., and Lazdunski, M. (1987). Purification and subunit structure of the [3H]phenamil receptor associated with the renal apical Na⁺ channel. *Proc. Natl. Acad. Sci. USA* **84**, 4836–4840.
14. Lingrel, J.B., Arguello, J.M., Van Huysse, J., and Kuntzweiler, T.A. (1997). Cation and cardiac glycoside binding sites of the Na,K-ATPase. *Ann. N Y Acad. Sci.* **834**, 194–206.
15. Inukai, K., Asano, T., Katagiri, H., Anai, M., Funaki, M., Ishihara, H., Tsukada, K., Kikuchi, M., Yazaki, Y., and Oka, Y. (1994). Replacement of both tryptophan residues at 388 and 412 completely abolished cytochalasin B photolabelling of the GLUT1 glucose. *Biochem. J.* **302**, 355–361.
16. Garcia, J.C., Strube, M., Leingang, K., Keller, K., and Mueckler, M.M. (1992). Amino acid substitutions at tryptophan 388 and tryptophan 412 of the HepG2 (Glut1) glucose transporter inhibit transport activity and targeting to the plasma membrane in *Xenopus* oocytes. *J. Biol. Chem.* **267**, 7770–7776.
17. Gutierrez, J.A., and Wessling-Resnick, M. (1996). Molecular mechanisms of iron transport. *Crit. Rev. Eukaryot. Gene Expr.* **6**, 1–14.
18. Nunez, M.T., Gaete, V., Watkins, J.A., and Glass, J. (1990). Mobilization of iron from endocytic vesicles. The effects of acidification and reduction. *J. Biol. Chem.* **265**, 6688–6692.
19. Watkins, J.A., Nunez, M.T., Gaete, V., Alvarez, O., and Glass, J. (1991). Kinetics of iron passage through subcellular compartments of rabbit reticulocytes. *J. Membr. Biol.* **119**, 141–149.
20. Oshiro, S., Nakajima, H., Markello, T., Krasnewich, D., Bernardini, I., and Gahl, W.A. (1993). Redox, transferrin-independent, and receptor-mediated endocytosis iron uptake systems in cultured human fibroblasts. *J. Biol. Chem.* **268**, 21586–21591.
21. Fleming, M.D., Romano, M.A., Su, M.A., Garrick, L.M., Garrick, M.D., and Andrews, N.C. (1998). Nramp2 is mutated in the anemic Belgrade (b) rat: evidence of a role for Nramp2 in endosomal iron transport. *Proc. Natl. Acad. Sci. USA* **95**, 1148–1153.
22. Fleming, M.D., Trenor, C.C., 3rd, Su, M.A., Foerzler, D., Beier, D.R., Dietrich, W.F., and Andrews, N.C. (1997). Microcytic anaemia mice have a mutation in Nramp2, a candidate iron transporter gene. *Nat. Genet.* **16**, 383–386.
23. Gunshin, H., Mackenzie, B., Berger, U.V., Gunshin, Y., Romero, M.F., Boron, W.F., Nussberger, S., Gollan, J.L., and Hediger, M.A. (1997). Cloning and characterization of a mammalian proton-coupled metal-ion transporter. *Nature* **388**, 482–488.
24. Bowen, B.J., and Morgan, E.H. (1987). Anemia of the Belgrade rat: evidence for defective membrane transport of iron. *Blood* **70**, 38–44.
25. Edwards, J.A., Sullivan, A.L., and Hoke, J.E. (1980). Defective delivery of iron to the developing red cell of the Belgrade laboratory rat. *Blood* **55**, 645–648.
26. Farcich, E.A., and Morgan, E.H. (1992). Diminished iron acquisition by cells and tissues of Belgrade laboratory rats. *Am. J. Physiol.* **262**, R220–R224.
27. Farcich, E.A., and Morgan, E.H. (1992). Uptake of transferrin-bound and nontransferrin-bound iron by reticulocytes from the Belgrade laboratory rat: comparison with Wistar rat transferrin and reticulocytes. *Am. J. Hematol.* **39**, 9–14.
28. Garrick, M.D., Gniecko, K., Liu, Y., Cohan, D.S., and Garrick, L.M. (1993). Transferrin and the transferrin cycle in Belgrade rat reticulocytes. *J. Biol. Chem.* **268**, 14867–14874.
29. Su, M.A., Trenor, C.C., Fleming, J.C., Fleming, M.D., and Andrews, N.C. (1998). The G185R mutation disrupts function of the iron transporter Nramp2. *Blood* **92**, 2157–2163.
30. Gruenheid, S., Canonne-Hergaux, F., Gauthier, S., Hackam, D.J., Grinstein, S., and Gros, P. (1999). The iron transport protein NRAMP2 is an integral membrane glycoprotein that colocalizes with transferrin in recycling endosomes. *J. Exp. Med.* **189**, 831–841.
31. Wessling-Resnick, M. (2000). Iron transport. *Annu. Rev. Nutr.* **20**, 129–151.
32. Inman, R.S., and Wessling-Resnick, M. (1993). Characterization of transferrin-independent iron transport in K562 cells. Unique properties provide evidence for multiple pathways of iron uptake. *J. Biol. Chem.* **268**, 8521–8528.
33. Simpson, R.J., and Peters, T.J. (1984). Studies of Fe³⁺ transport across isolated intestinal brush-border membrane of the mouse. *Biochim. Biophys. Acta* **772**, 220–226.
34. Sturrock, A., Alexander, J., Lamb, J., Craven, C.M., and Kaplan, J. (1990). Characterization of a transferrin-independent uptake system for iron in HeLa cells. *J. Biol. Chem.* **265**, 3139–3145.
35. Barisani, D., Berg, C.L., Wessling-Resnick, M., and Gollan, J.L. (1995). Evidence for a low Km transporter for non-transferrin-bound iron in isolated rat hepatocytes. *Am. J. Physiol.* **269**, G570–G576.
36. Kaplan, J., Jordan, I., and Sturrock, A. (1991). Regulation of the transferrin-independent iron transport system in cultured cells. *J. Biol. Chem.* **266**, 2997–3004.
37. Morgan, E.H. (1988). Membrane transport of non-transferrin-bound iron by reticulocytes. *Biochim. Biophys. Acta* **943**, 428–439.
38. Gutteridge, J.M., Rowley, D.A., Griffiths, E., and Halliwell, B. (1985). Low-molecular-weight iron complexes and oxygen radical reactions in idiopathic haemochromatosis. *Clin. Sci. (Lond.)* **68**, 463–467.
39. Batey, R.G., Lai Chung Fong, P., Shamir, S., and Sherlock, S. (1980). A non-transferrin-bound serum iron in idiopathic hemochromatosis. *Dig. Dis. Sci.* **25**, 340–346.
40. Cabantchik, Z.I., Glickstein, H., Milgram, P., and Breuer, W. (1996). A fluorescence assay for assessing chelation of intracellular iron in a membrane model system and in mammalian cells. *Anal. Biochem.* **233**, 221–227.
41. Zanninelli, G., Glickstein, H., Breuer, W., Milgram, P., Brissot, P., Hider, R.C., Konijn, A.M., Libman, J., Shanzer, A., and Cabantchik, Z.I. (1997). Chelation and mobilization of cellular iron by different classes of chelators. *Mol. Pharmacol.* **51**, 842–852.
42. Breuer, W., Epsztejn, S., Millgram, P., and Cabantchik, I.Z. (1995). Transport of iron and other transition metals into cells as revealed by a fluorescent probe. *Am. J. Physiol.* **268**, 1354–1361.
43. Breuer, W., Epsztejn, S., and Cabantchik, Z.I. (1995). Iron acquired from transferrin by K562 cells is delivered into a cytoplasmic pool of chelatable iron(II). *J. Biol. Chem.* **270**, 24209–24215.
44. Staubli, A., and Boelsterli, U.A. (1998). The labile iron pool in hepatocytes: prooxidant-induced increase in free iron precedes oxidative cell injury. *Am. J. Physiol.* **274**, 1031–1037.
45. Pinerio, D.J., Hu, J., Cook, B.M., Scaduto, R.C., Jr., and Connor, J.R. (2000). Interleukin-1beta increases binding of the iron regulatory protein and the synthesis of ferritin by increasing the labile iron pool. *Biochim. Biophys. Acta* **1497**, 279–288.
46. Schonhorn, J.E., Akompong, T., and Wessling-Resnick, M. (1995). Mechanism of transferrin receptor down-regulation in K562 cells in response to protein kinase C activation. *J. Biol. Chem.* **270**, 3698–3705.
47. Schonhorn, J.E., and Wessling-Resnick, M. (1994). Brefeldin A down-regulates the transferrin receptor in K562 cells. *Mol. Cell. Biochem.* **135**, 159–169.
48. Hynes, J., Floyd, S., Soini, A.E., O'Connor, R., and Papkovsky, D.B. (2003). Fluorescence-based cell viability screening assays using water-soluble oxygen probes. *J. Biomol. Screen.* **8**, 264–272.
49. Yang, A., Cardona, D.L., and Barile, F.A. (2002). In vitro cytotoxicity testing with fluorescence-based assays in cultured human lung and dermal cells. *Cell Biol. Toxicol.* **18**, 97–108.
50. Greger, R. (1990). Chloride channel blockers. *Methods Enzymol.* **191**, 793–810.
51. Tunnickliff, G., and Smith, J.A. (1981). Competitive inhibition of gamma-aminobutyric acid receptor binding by N-2-hydroxyethylpiperazine-N'-2-e-ethanesulfonic acid and related buffers. *J. Neurochem.* **36**, 1122–1126.
52. Matheson, G.K., Freed, E., and Tunnickliff, G. (1986). Novel GABA analogues as hypotensive agents. *Neuropharmacology* **25**, 1191–1195.
53. Davis-Kaplan, S.R., Askwith, C.C., Bengtzen, A.C., Radisky, D., and Kaplan, J. (1998). Chloride is an allosteric effector of copper assembly for the yeast multicopper oxidase Fet3p: an unexpected role for intracellular chloride channels. *Proc. Natl. Acad. Sci. USA* **95**, 13641–13645.

54. Ponka, P., Borova, J., Neuwirt, J., Fuchs, O., and Necas, E. (1979). A study of intracellular iron metabolism using pyridoxal isonicotinoyl hydrazone and other synthetic chelating agents. *Biochim. Biophys. Acta* 586, 278–297.
55. Ponka, P., Borova, J., Neuwirt, J., and Fuchs, O. (1979). Mobilization of iron from reticulocytes. Identification of pyridoxal isonicotinoyl hydrazone as a new iron chelating agent. *FEBS Lett.* 97, 317–321.
56. Nick, H., Wong, A., Acklin, P., Faller, B., Jin, Y., Lattmann, R., Sergejew, T., Hauffe, S., Thomas, H., and Schnebli, H.P. (2002). ICL670A: preclinical profile. *Adv. Exp. Med. Biol.* 509, 185–203.